Journal of Solid State Chemistry 181 (2008) 2346–2349

Contents lists available at ScienceDirect

Journal of Solid State Chemistry

journal homepage: www.elsevier.com/locate/jssc

Flux growth and magnetic properties of $FeVO_4$ single crystals

Zhangzhen He*, Jun-Ichi Yamaura, Yutaka Ueda

Institute for Solid State Physics, University of Tokyo, Kashiwa, Chiba 277-8581, Japan

ARTICLE INFO

Article history:
Received 7 April 2008
Received in revised form
26 May 2008
Accepted 27 May 2008
Available online 4 June 2008

Keywords:
$FeVO_4$
Crystal growth
Antiferromagnet
Two magnetic orderings

ABSTRACT

$FeVO_4$ (**I**) single crystals are grown by the flux method using V_2O_5 as the self-flux. The grown crystals exhibit a characteristic morphology with natural facets. The quality of the crystals is confirmed by X-ray diffraction and EPMA techniques. Magnetic properties are investigated by means of magnetic susceptibility, magnetization, and heat capacity measurements. Two magnetic phase transitions are observed at ~13 and ~20 K. Such unusual magnetic behaviors are suggested to originate from two different Fe ligand environments of octahedral FeO_6 and trigonal bipyramidal FeO_5 in a six-column doubly bent chain.

1. Introduction

$FeVO_4$ (Fe^{3+} and V^{5+}) has four different polymorphs that exhibit a rich structure chemistry. $FeVO_4$ (form-**I**) crystallizes in a triclinic system with space group $P\bar{1}$, while other forms (-**II**, -**III**, and -**IV**) crystallize in the orthorhombic $CrVO_4$ structure, the orthorhombic α-PbO_2 structure, and the monoclinic wolframite $NiWO_4$ structure, respectively [1–3]. It is reported that triclinic $FeVO_4$ (**I**) is only one stable phase at the ambient condition, while other metastable phases (-**II**, -**III**, and -**IV**) are usually formed at the high-pressure and high-temperature conditions [1]. The structure of triclinic $FeVO_4$ (**I**) [4] has been determined using a single crystal, showing a peculiar chain structure (Fig. 1a). Fe^{3+} ions have three independent crystallographic sites, of which two sites are in distorted octahedral FeO_6 and one site is in a distorted trigonal bipyramidal FeO_5 environment. Fe–O polyhedra form an interesting six-column doubly bent chain via edge-sharing (Fig. 1b) and the chains are joined by VO_4 tetrahedra to form a three-dimensional framework. On the other hand, magnetic behaviors of $FeVO_4$ (**I**) have been investigated by means of susceptibility and heat capacity measurements in the past decades, showing an antiferromagnetic ordering at ~22 K [5] or two magnetic orderings at 15.6 and 21 K [6]. However, previous magnetic measurements were focused on powdered samples, due to the growth of frequently twinned crystals and/or lack of large-sized single crystals. Therefore, a large-sized single crystal of $FeVO_4$ (**I**) with good quality is expected to elucidate its true magnetic nature.

Recently we have established a closed system for flux growth of many vanadium oxides [7–9]. In this study, large-sized $FeVO_4$ (**I**) single crystals with high quality are grown in a closed crucible by the flux method using V_2O_5 as the self-flux and its magnetic behaviors are investigated along different crystallographic directions by means of susceptibility, magnetization, and heat capacity measurements. Our results confirm that $FeVO_4$ (**I**) single crystals exhibit interesting magnetic properties in which two magnetic phase transitions occur at 13 and 20 K.

2. Experimental section

A mixture of high-purity reagents of $FeC_2O_4 \cdot 2H_2O$ (3 N, 25.0 g) and V_2O_5 (4 N, 25.3 g) was ground carefully and homogenized thoroughly with ethanol (99%) in an agate mortar. The mixture was packed into an alumina crucible ($\Phi 42 \times 50\,mm^3$) and then the crucible was capped with a cover using Al_2O_3 cement (C-989, Cotronics Corp.). Such closed crucible was put into a homemade electric furnace with an adjustable temperature gradient and then the furnace was heated up to 980 °C and kept at 980 °C for 10 h to ensure that the solution melts completely and homogeneously. The furnace was cooled slowly down to 600 °C at a rate of 1 °C/h while keeping at a constant temperature several times, and then cooled down to room temperature at a rate of about 100 °C/h. With this procedure, dark red crystals were obtained by mechanical separation from the crucible.

The X-ray powder diffraction (XRD) data were collected at room temperature in the range $2\theta = 10$–80° with a scan step width of 0.02° and a fixed counting time of 4 s using an

---

* Corresponding author. Present address: Fujian Institute of Research on the Structure of Matter, Chinese Academy of Sciences, Fuzhou, Fujian 350002, People's Republic of China. Fax: +86 591 83799252.
E-mail addresses: hezz@fjirsm.ac.cn, he@issp.u-tokyo.ac.jp, hcz1988@hotmail.com (Z. He).

0022-4596/$ - see front matter © 2008 Elsevier Inc. All rights reserved.
doi:10.1016/j.jssc.2008.05.041

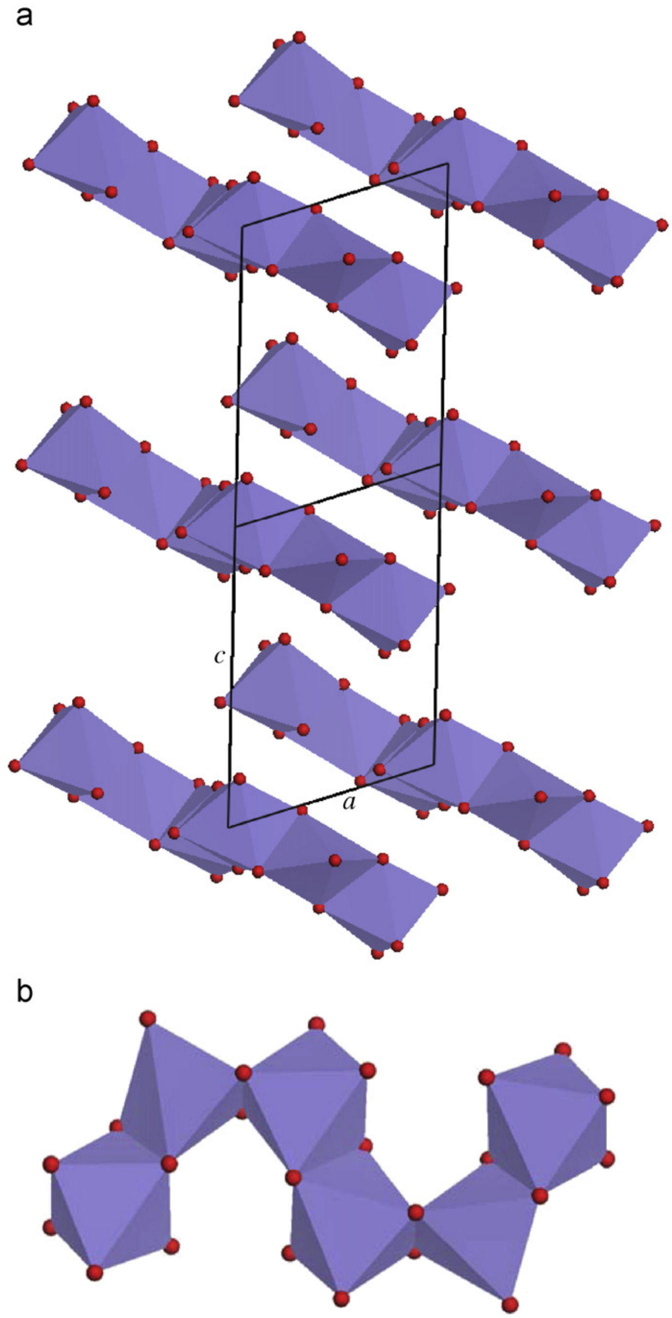

Fig. 1. (a) A peculiar chain structure of $FeVO_4$ built by Fe–O polyhedra and (b) the form of a six-column doubly bent chain.

MXP21AHF (Mac Science) powder diffractometer with graphite monochromatized Cu$K\alpha$ radiation. Chemical analysis was performed using an electron probe microanalysis (EPMA) system (JEOL JSM-5600 · Oxford Link ISIS). Magnetic susceptibility and magnetization were measured using a superconducting quantum interference device (MPMS-5S, Quantum Design) magnetometer and heat capacity was measured by a relaxation method using a commercial Physical Property Measurement System (PPMS, Quantum Design).

3. Results and discussion

Fig. 2(a) shows the grown crystals and their morphology. It was found that all of the grown crystals exhibit a characteristic pillar-like morphology with clear growth facets. Fig. 2(b) shows an enlarged view of a crystal. The cleaved facets are confirmed to be $(0\bar{1}\bar{1})$, $(00\bar{1})$, $(01\bar{1})$, and $(2\bar{1}0)$ planes and no twinned feature can be detected using a Bruker SMART three-circle diffractometer equipped with a CCD area detector, showing that the long direction of the grown crystals is the a-axis. The grown crystals were analyzed by XRD and EPMA techniques. It was found that all peaks in the XRD pattern can be indexed with the triclinic system and identified to diffraction peaks from $FeVO_4$ (Ref: ICSD Code 10329). No impurity phases were detected. The lattice constants of $a = 6.709(3)$ Å, $b = 8.045(3)$ Å, $c = 9.340(3)$ Å, $\alpha = 96.43(2)^\circ$, $\beta = 106.85(1)^\circ$, and $\gamma = 101.49(2)^\circ$ determined by the single-crystal XRD technique are in good agreement with those reported previously in Ref. [4]. In addition, chemical analysis with the EDS spectrum performed using an EPMA system indicated that no other metal elements except for Fe and V were detected and the molar ratio of Fe:V was calculated to be approximately 1:1, agreeing with the formula of $FeVO_4$. These results clearly show that the grown crystals are triclinic $FeVO_4$ (**I**) and have high quality.

Since $FeVO_4$ exhibits an incongruent melting feature based on the phase diagrams of the Fe_2O_3–V_2O_5 system [10], the flux method is expected for growth of $FeVO_4$ single crystals. To avoid impurity from flux into the grown crystals, we selected one of starting materials V_2O_5 to be self-flux. The molar ratio of Fe_2O_3:$V_2O_5 = 1:2$, which corresponds to that of $FeVO_4$:$V_2O_5 = 1:1$, is considered in this study. As discussed in Refs. [7–9], to grow large $FeVO_4$ single crystals with high quality, a detailed growth process is noted as follows: to prevent the formation of excess nucleation in the system and to allow slow spontaneous nucleation only at the surface of the melt, the growth was carried out under a higher vertical temperature gradient of 100 °C/cm at a very slow cooling rate of 1 °C/h. Further, to avoid the inclusions of the melt into the crystal due to overcool of the melt, the furnace was kept at a constant temperature several times in the cooling process. In addition, to carefully avoid the evaporation of V_2O_5 at high temperature resulting in an unsteady solution system during the growth, the alumina crucible was capped with a cover using Al_2O_3 cement to be a closed system.

Fig. 3 shows the temperature dependence of magnetic susceptibility and corresponding reciprocal susceptibility measured in an applied field 0.1 T along the a-axis from 5 to 300 K on heating. A sharp peak is observed at ~20 K, indicating the onset of antiferromagnetic (AF) ordering. Above 30 K, a typical Curie–Weiss behavior is observed, giving the Curie constant $C = 4.250(9)$ emu K/mol and Weiss constant $\theta = -97.36(8)$ K. The effective magnetic moment (μ_{eff}) is calculated to be $5.831(5)\,\mu_B$, which is close to the value of $5.91(6)\,\mu_B$ for $S = 5/2$ with a g factor of 2, showing that Fe^{3+} ions have a high spin state. Also, the negative Weiss constant suggests that the interactions between Fe^{3+} ions are AF.

Fig. 4 shows magnetic susceptibilities along different directions. Two anomalies at ~20 and ~13 K are clearly seen in susceptibilities measured in an applied field perpendicular to $(0\bar{1}\bar{1})$, $(00\bar{1})$, and $(01\bar{1})$ planes, which are different from only one peak in susceptibility along the a-axis. The result indicates the appearance of two magnetic orderings at low temperature. Fig. 5 shows magnetization (M) as a function of applied field (H) at $T = 5$ K. A linear increase in magnetization is observed in the applied field parallel to the a-axis and perpendicular to the $(00\bar{1})$ and $(01\bar{1})$ planes, agreeing with the AF ordering below 13 K, while a slight increase is observed at around $H = \sim 3.5$ T perpendicular to the $(0\bar{1}\bar{1})$ plane, presumably indicating a field-induced spin-flop transition.

Fig. 6 shows heat capacity data in an applied field of $H = 0$. There are two clear signs of a λ-like feature around 13 and 20 K,

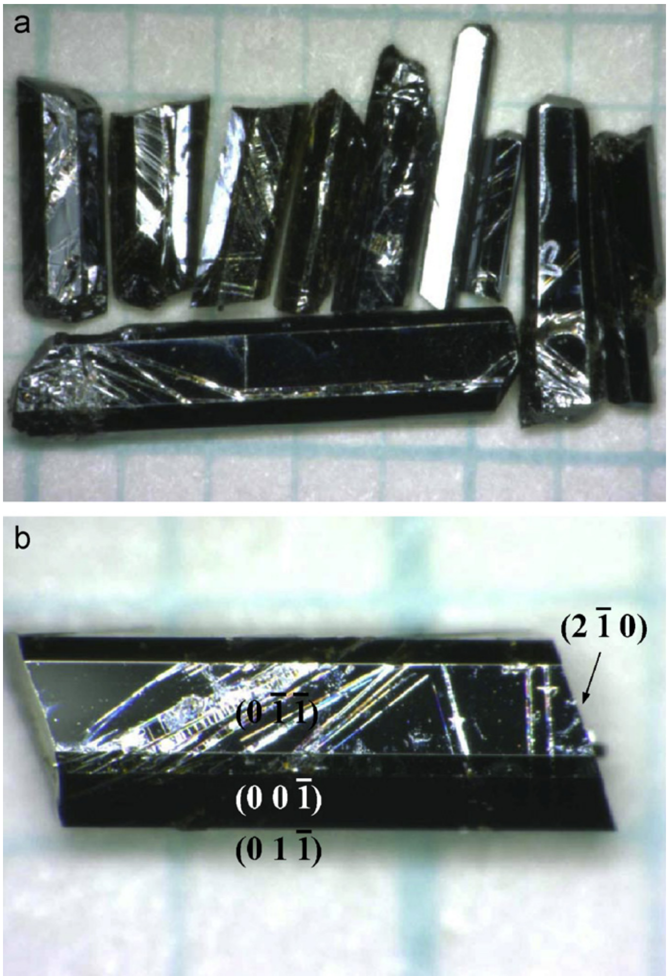

Fig. 2. (a) $FeVO_4$ single crystals with a characteristic morphology and (b) an enlarged view of a crystal.

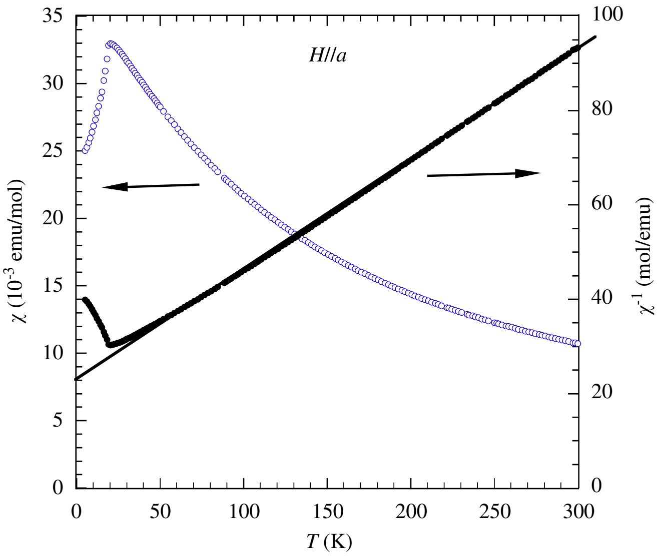

Fig. 3. Magnetic susceptibility and reciprocal one of $FeVO_4$ measured in a magnetic field of 0.1 T along the *a*-axis.

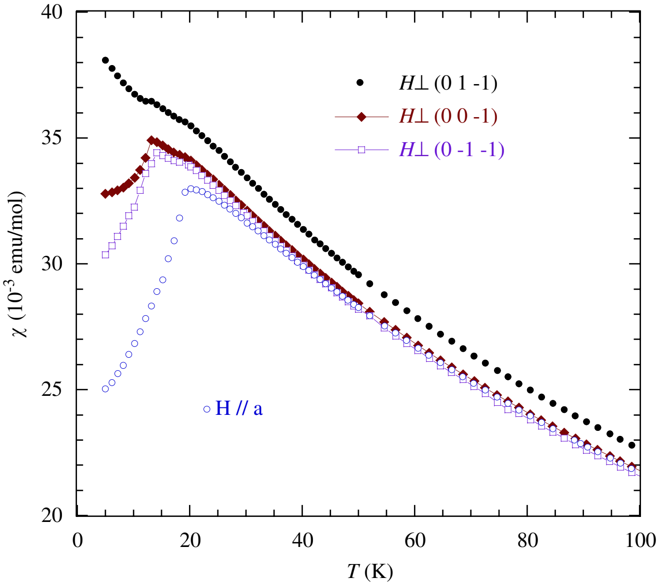

Fig. 4. Magnetic susceptibility measured in an applied field parallel to the *a*-axis and perpendicular to the $(0\bar{1}\bar{1})$, $(00\bar{1})$, and $(01\bar{1})$ planes of the $FeVO_4$ single crystal.

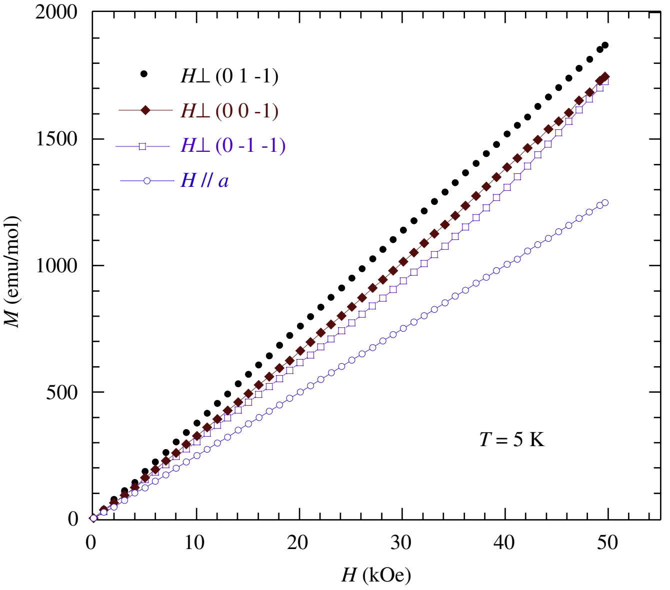

Fig. 5. Magnetization (*M*) as a function of magnetic field (*H*) applied parallel to the *a*-axis and perpendicular to the $(0\bar{1}\bar{1})$, $(00\bar{1})$, and $(01\bar{1})$ planes of the $FeVO_4$ single crystal.

which correspond to the temperature of anomalies in the magnetic susceptibilities, giving clear evidence of two AF long-range orderings. This is in good agreement with those reported previously on polycrystalline samples [6]. In addition, since $FeVO_4$ is an insulator, the total heat capacity *C* can be considered as the sum of the lattice term (C_l) and the magnetic term (C_m), $C_p = \gamma T + \beta T^3$, where γT corresponds to the magnetic contribution C_m from spin systems and βT^3 to the lattice one C_l from phonons. As shown in Fig. 6(b), heat capacity data above 30 K can be fitted well with $\gamma = 0.289(3)\,\mathrm{J\,mol^{-1}\,K^{-1}}$ and $\beta = 2.727(6)\times10^{-5}\,\mathrm{J\,mol^{-1}\,K^{-4}}$. The β value gives a Debye temperature of 773.1(7) K. The magnetic contribution can be calculated as $C_m = C_p - C_l$ and the magnetic entropy integrated over λ-like anomalies at ~20 and ~13 K are estimated to be $\Delta S = {\sim}2.284(3)$ and ${\sim}0.156(8)\,\mathrm{J\,mol^{-1}\,K^{-1}}$, respectively, which corresponds to approximately 17.1% of $R\ln(2S+1)$ expected for spin-5/2 systems in overall. The change in magnetic entropy at

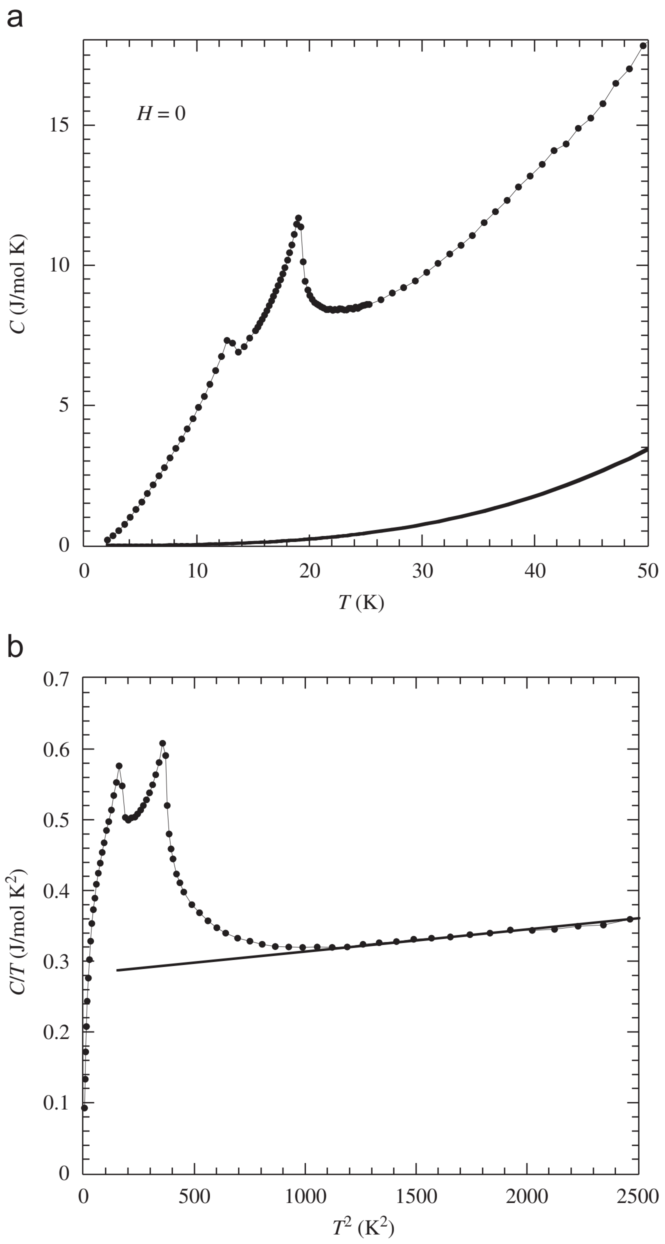

Fig. 6. (a) Heat capacity (C_p) measured in zero magnetic field. The solid line represents the lattice contribution (C_l). (b) The plot of C_p/T vs T^2.

~13 K is much smaller than that at ~20 K, indicating most of the entropy of the system is lost through the magnetic correlation at a higher temperature.

Our experimental results of the magnetic susceptibility and heat capacity confirmed that triclinic $FeVO_4$ (**I**) exhibits two long-range magnetic orderings at low temperature. Such interesting multiple magnetic phase transitions may originate from two completely decoupled magnetic subsystems in the system as seen in $Ni_2FeO_2BO_3$ [11] or competing magnetic interactions as seen in $Ni_3V_2O_8$ and $Co_3V_2O_8$ [12–15]. We suggest that two long-range magnetic orderings in triclinic $FeVO_4$ (**I**) may be closely related to two different Fe ligand environments of octahedral FeO_6 and trigonal bipyramidal FeO_5 in a six-column doubly bent chain. However, further studies including neutron scattering are needed to understand the magnetic nature of $FeVO_4$.

4. Conclusions

Large triclinic $FeVO_4$ (**I**) single crystals with a characteristic morphology have been successfully grown by the flux method using V_2O_5 as the self-flux. The grown crystals were confirmed to have good quality by XRD and EPMA techniques. Magnetic properties have been investigated by means of magnetic susceptibility, magnetization, and heat capacity measurements, showing that triclinic $FeVO_4$ (**I**) exhibits two magnetic orderings at ~20 and ~13 K. We suggested that such interesting multiple magnetic transitions in triclinic $FeVO_4$ (**I**) are related to two different Fe ligand environments of octahedral FeO_6 and trigonal bipyramidal FeO_5 in a six-column doubly bent chain.

Acknowledgment

One of the authors (Z. H.) acknowledges the Japan Society for the Promotion of Science (JSPS) for awarding the Foreigner Postdoctoral Fellowship (P06047).

References

[1] J. Muller, J.C. Joubert, J. Solid State Chem. 14 (1975) 8.
[2] A.P. Young, C.M. Schwartz, Acta Crystallogr. 15 (1962) 1305.
[3] F. Laves, Acta Crystallogr. 17 (1964) 1476.
[4] B. Robertson, E. Kostiner, J. Solid State Chem. 4 (1972) 29.
[5] L.M. Levinson, B.M. Wanklyn, J. Solid State Chem. 3 (1971) 131.
[6] V.I. Surikov, V.N. Lisson, V.I. Surikov, N.I. Kourov, Fizika Nizkikh Temperatur (Kiev) 9 (1983) 1109.
[7] Z. He, Y. Ueda, J. Cryst. Growth 310 (2008) 171.
[8] Z. He, Y. Ueda, Cryst. Growth Des. 8 (7) (2008), in press (available online).
[9] Z. He, J. Yamaura, Y. Ueda, Cryst. Growth Des. 8 (2008) 799.
[10] E.M. Levin, C.R. Robbins, H.F. Mcmurdie, Phase Diagrams for Ceramists, No. 96, American Ceramic Society, Westerville, OH, 1964.
[11] J.C. Fernandes, R.B. Guimaraes, M.A. Continentino, H.A. Borges, A. Sulpice, J.L. Tholence, J.L. Siqueira, L.I. Zawislak, J.B.M.C.A. dos Santos, Phys. Rev. B 58 (1998) 287.
[12] N. Rogado, G. Lawes, D.A. Huse, A.P. Ramirez, R.J. Cava, Solid State Commun. 124 (2002) 229.
[13] G. Lawes, M. Kenzelmann, N. Rogado, K.H. Kim, G.A. Jorge, R.J. Cava, A. Aharony, O. Entin-Wohlman, A.B. Harris, T. Yildirim, Q.Z. Huang, S. Park, C. Broholm, A.P. Ramirez, Phys. Rev. Lett. 93 (2004) 247201.
[14] M. Kenzelmann, A.B. Harris, A. Aharony, O. Entin-Wohlman, T. Yildirim, Q. Huang, S. Park, G. Lawes, C. Broholm, N. Rogado, R.J. Cava, K.H. Kim, G. Jorge, A.P. Ramirez, Phys. Rev. B 74 (2006) 014429.
[15] Y. Chen, W.J. Lynn, Q. Huang, F.M. Woodward, T. Yildirim, G. Lawes, A.P. Ramirez, N. Rogado, R.J. Cava, A. Aharony, O. Entin-Wohlman, A.B. Harris, Phys. Rev. B 74 (2006) 014430.